

## Selective Sorption of Nanoporous Poly(methyl silsesquioxane)

Ho-Cheol Kim,\* Jason B. Wilds, William D. Hinsberg, Larry R. Johnson, Willi Volksen, Teddie Magbitang, Victor Y. Lee, James L. Hedrick, Craig J. Hawker, and Robert D. Miller\*

IBM Almaden Research Center, 650 Harry Road, San Jose, California 95120-6099

Elbert Huang

IBM T. J. Watson Research Center, Yorktown Heights, New York 10595

Received April 10, 2002. Revised Manuscript Received September 20, 2002

The sorption behavior of nanoporous poly(methyl silsesquioxane), PMSSQ, thin films was investigated using a quartz crystal microbalance (QCM) combined with reflectance infrared spectroscopy (IR). The nanoporous PMSSQ films are intrinsically hydrophobic and show highly selective sorption behavior. With organic liquids having surface tensions below the critical value (38–48 dyn/cm), the extent of sorption increased with porosity of PMSSQ films. Extremely low amounts of sorption were measured with liquids having a surface tension higher than the critical value. The selective sorption behavior can be interpreted by capillary condensation resulting from the lowered vapor pressure in the nanoscopic pores.

### Introduction

Sorption behavior of a gas (or a vapor in equilibrium with liquid) on a clean solid surface is a common and well-understood phenomenon. The extent of sorption at equilibrium depends on temperature, the pressure of the gas (or vapor), and the effective surface area of the solid. Numerous experimental and theoretical studies have been done to reveal the relationship among those parameters for various gas (vapor)/solid combinations.<sup>1</sup> Recently of interest is the sorption behavior of porous substrates whose pore sizes span the so-called *meso*-size range (2–50 nm by IUPAC definition).<sup>2</sup> Because of the nanoscopic length scale of the pores, the porous substrates, hereafter referred to as *nano*porous films, have extremely high air/film interfacial area which provides significantly more sites to adsorb gas (or vapor) than dense solid films. In addition, capillary condensation can take place in the nanopores at pressures far lower than the normal saturation vapor pressures.

The generation of nanoporous materials is nontrivial. Since Kresge et al.<sup>3</sup> and Beck et al.<sup>4</sup> reported surfactant-templated nanoporous silicates, much experimental effort has been devoted to investigating the unique

sorption properties of nanoporous materials. However, the organic modification steps necessary to overcome the inherent limitations such as low hydrothermal stability and low reactivity are known to limit the fabrication of nanoporous materials. Recently, supercritical fluids have been used to generate nanoporous films, but the control of size and morphology is still restricted.<sup>5</sup>

A simple and highly efficient route to nanoporous organic or inorganic films has been developed at IBM.<sup>6</sup> In this approach, thin films of nanoporous organosilicates were obtained by inducing phase separation of macromolecular porogens (pore-generators) in blends with inorganic matrix polymers and subsequent thermal decomposition of the porogen phase. Extensive studies on the use of nanoporous PMSSQ as low dielectric constant (*k*) materials have been done since nanoporous films have been recognized as a viable route to low *k* materials for intermetal dielectrics. In addition to the dielectric constant, low moisture uptake is an important requirement for real on-chip applications of nanoporous materials. For Al-alloy (gap-fill) and Cu (damascene)

(5) Krause, B.; Sijbesma, H. J. P.; Münüklü, P.; van der Vegt, N. F. A.; Wessling, M. *Macromolecules* **2001**, *34*, 8792.

(6) (a) Hedrick, J. L.; Labadie, J.; Russell, T. P.; Hofer, D.; Wakharker, V. *Polymer* **1993**, *34*, 4717. (b) Miller, R. D.; Hedrick, J. L.; Yoon, D. Y.; Cook, R. F.; Hummel, J. P. *MRS Bull.* **1997**, *22*, 44. (c) Hedrick, J. L.; Miller, R. D.; Hawker, C. J.; Carter, K. R.; Volksen, W.; Yoon, D. Y.; Trollsas, M. *Adv. Mater.* **1998**, *10*, 1049. (d) Hedrick, J. L.; Hawker, C. J.; Trollsas, M.; Remenar, J.; Yoon, D. Y.; Miller, R. D. *Mater. Res. Symp. Proc.* **1998**, *519*, 65. (e) Miller, R. D. *Science* **1999**, *286*, 412. (f) Nguyen, C. V.; Carter, K. R.; Hawker, C. J.; Hedrick, J. L.; Jaffe, R. L.; Miller, R. D.; Remenar, J. F.; Rhee, H.-W.; Rice, P. M.; Toney, M. F.; Trollsas, M.; Yoon, D. Y. *Chem. Mater.* **1999**, *11*, 3080. (g) Hawker, C. J.; Hedrick, J. L.; Miller, R. D.; Volksen, W. *MRS Bull.* **2000**, *25*, 54. (h) Nguyen, C.; Hawker, C. J.; Miller, R. D.; Huang, E.; Hedrick, J. L.; Gauderon, R.; Hilborn, J. G. *Macromolecules* **2000**, *33*, 4281. (i) Heise, A.; Nguyen, C.; Malek, R.; Hedrick, J. L.; Frank, C. W.; Miller, R. D. *Macromolecules* **2000**, *33*, 2346. (j) Mecerreyes, D.; Huang, E.; Magbitang, T.; Volksen, W.; Hawker, C. J.; Lee, V.; Miller, R. D.; Hedrick, J. L. *High Perform. Polym.* **2001**, *13*, 11.

\* Authors to whom correspondence should be addressed: hckim@us.ibm.com (e-mail), 408-927-3725 (phone), 408-927-3310 (fax); or rdmiller@almaden.ibm.com (e-mail), 408-927-1646 (phone), 408-927-3310 (fax).

(1) Adamson, A. W.; Gast, A. P. *Physical Chemistry of Surfaces*; John Wiley & Sons: New York, 1997.

(2) Stein, A.; Melde, B. J.; Schroden, R. C. *Adv. Mater.* **2000**, *12*, 1403, and references therein.

(3) Kresge, C. T.; Leonowicz, M. E.; Roth, W. J.; Vartuli, J. C.; Beck, J. S. *Nature* **1992**, *359*, 710.

(4) Beck, J. S.; Vartuli, J. C.; Roth, W. J.; Leonowicz, M. E.; Kresge, C. T.; Schmitt, K. D.; Chu, C. T.-W.; Olson, D. H.; Sheppard, E. W.; McCullen, S. B.; Higgins, J. B.; Schlenker, J. L. *J. Am. Chem. Soc.* **1992**, *114*, 10834.

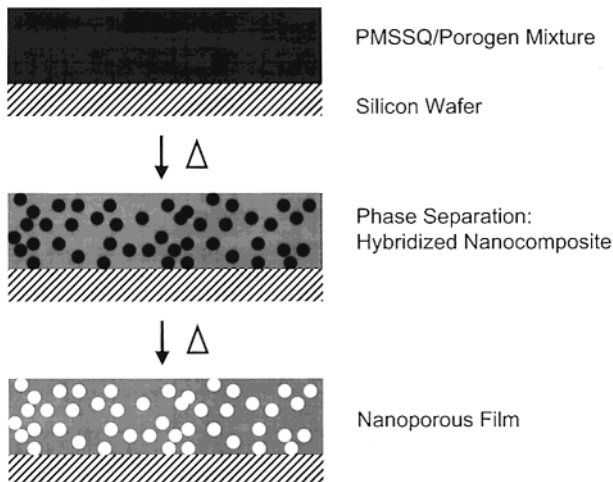


**Figure 1.** Schematic sketch for generation of nanoporous PMSSQ films from phase-separated inorganic–organic hybrids.

integration, moisture sorption must be less than 2 wt % at 100% relative humidity.<sup>7</sup> It is crucial, therefore, to understand the sorption behavior of nanoporous films from both a scientific and technological point of view.

In this article, we report the selective sorption behavior of nanoporous PMSSQ using a QCM combined with a reflectance infrared spectroscopy. The QCM is a fairly mature measurement method that is highly sensitive to mass changes in thin films. Under typical operating conditions, the minimum detectable mass change is approximately 10 ng/cm<sup>2</sup>.<sup>8</sup> As the observations discussed here will indicate, nanoporous PMSSQ films show highly selective sorption behavior for different organic liquids. This unique selectivity is expected to open up new possibilities for many interesting applications of nanoporous PMSSQ films.

## Experimental Section

**Preparation of Nanoporous Films.** The nanoporous PMSSQ films were prepared by the method presented schematically in Figure 1. PMSSQ was used as supplied from Dow Corning (Mw 15 000, determined by SEC analysis using linear polystyrene standards). Poly(methyl methacrylate-*co*-dimethyl amino ethyl methacrylate), P(MMA-*co*-DMAEMA), was used as the porogen for this study. P(MMA-*co*-DMAEMA) was synthesized by atom transfer radical polymerization (ATRP) (Mw 12 000, PDI 1.1).<sup>9</sup> Thin films of PMSSQ/porogen mixtures containing varying amounts of porogen were prepared by spin casting 1-methoxy-2-propanol (PMOH) solutions either on clean silicon wafers or on the Au electrode of AT-cut quartz crystals (MAXTEK, Inc., 5 MHz). Samples were heated to 450 °C at a ramp rate of 5 °C /min under an argon atmosphere to generate porous structure. Regarding elemental composition of nanoporous PMSSQ films, X-ray photoelectron spectroscopy (XPS) results show no difference between dense PMSSQ and nanoporous PMSSQ film at least within a few hundred angstroms from the air/film interface.<sup>10</sup> Film thicknesses and refractive indices were determined with a prism coupler (Meticon, model 2010) using a helium–neon laser ( $\lambda = 632.8$  nm). The nanoporous films are optically homogeneous and the

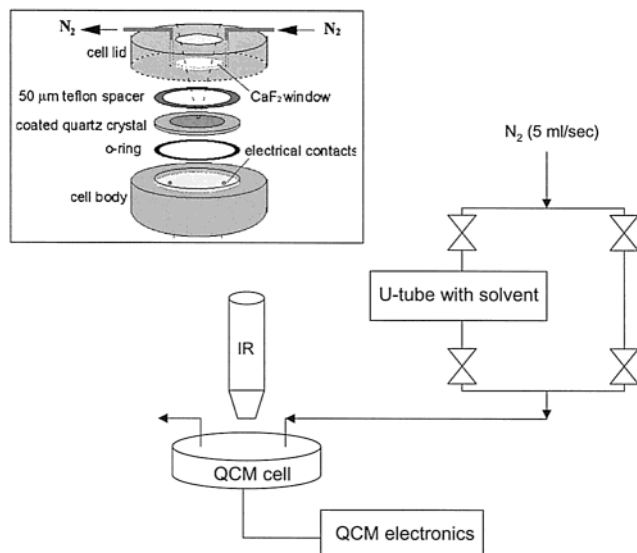


**Figure 2.** Diagram for QCM setup in this study. Inset shows the cell lid construction for reflectance IR measurements.

refractive index of the films decreases with increasing porogen loading. A field-emission scanning electron microscope (FES-EM) (Hitachi S-4700) was used to image the cross-sectional morphology of the films. Static water contact angles were measured with an AST video contact angle system 2500XE. Infrared spectra were acquired using a Nicolet Continuum infrared microscope configured for reflectance measurements and attached to a Nicolet Nexus 470 Fourier transform infrared spectrometer. The spectrometer was operated in rapid scan series mode, recording 16 spectra per minute with 64 scans per spectrum.

**QCM Measurements.** Mass uptake of nanoporous PMSSQ was determined with a custom-built QCM.<sup>11</sup> Mass changes can be calculated from the resonant frequency shifts ( $\Delta f$ ) of QCM using the Sauerbrey equation under the assumption that the transverse acoustic wave velocity associated with the porous thin films is identical to that of quartz

$$\Delta f = -2f_0^2 \frac{\Delta m}{A} (\mu_q \rho_q)^{1/2}$$

where,  $f_0$  is the frequency of bare quartz crystal,  $\Delta m$  is the mass change,  $A$  is the piezoelectrically active area of the Au electrode, and  $\rho_q$  and  $\mu_q$  represent the density and shear modulus of quartz, respectively.<sup>8</sup> The QCM setup for this study is shown in Figure 2. After the samples were placed into the QCM cell, they were exposed to either pure nitrogen (10 psi, 5 mL/sec; denoted as a desorption cycle) or nitrogen containing the vapor of an organic liquid (a sorption cycle) for a period of time. The duration of each desorption and sorption cycle was 5 min, and each measurement was composed of three sorption cycles separated by desorption cycles. The crystal frequency shift was recorded 5 times per second during the measurement. The ratio of frequency shifts was used to determine the percent sorption as follows:

$$\% \text{ sorption} = [(f_1 - f_2)/(f_0 - f_2)] \times 100$$

where  $f_1$  and  $f_2$  are the frequency of nanoporous PMSSQ before and after exposure to the vapor, respectively. The differences in densities of organic liquids were considered by normalizing with respect to the density of pure PMSSQ (1.2 g/cm<sup>3</sup>). IR reflectance spectra were obtained simultaneously with the QCM measurements by focusing the IR microscope, through a calcium fluoride window located in the QCM cell lid, onto the film layer on the crystal surface.

(7) Lee, W. W.; Ho, P. S. *MRS Bull.* **1997**, *22*, 19.

(8) Buttry, D. A.; Ward, M. D. *Chem. Rev.* **1992**, *92*, 1355.

(9) (a) Hawker, C. J.; Bosman, A. W.; Harth, E. *Chem. Rev.* **2001**, *101*, 3661. (b) Kamigaito, M.; Ando, T.; Sawamoto, M. *Chem. Rev.* **2001**, *101*, 3689.

(10) Huang, Q. R.; Frank, C. W.; Mecerreyres, D.; Miller, R. D. *Polym. Mater. Sci. Eng.* **2001**, *84*, 792.

(11) Lee, S.; Hinsberg, W. D.; Kanazawa, K. *Anal. Chem.* **2002**, *74*, 125.

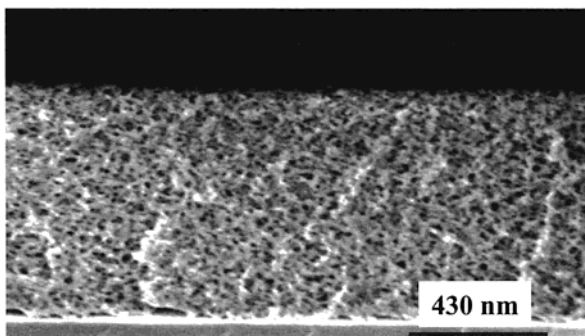


**Figure 3.** FESEM image of nanoporous PMSSQ films having 50 wt % porogen loading.

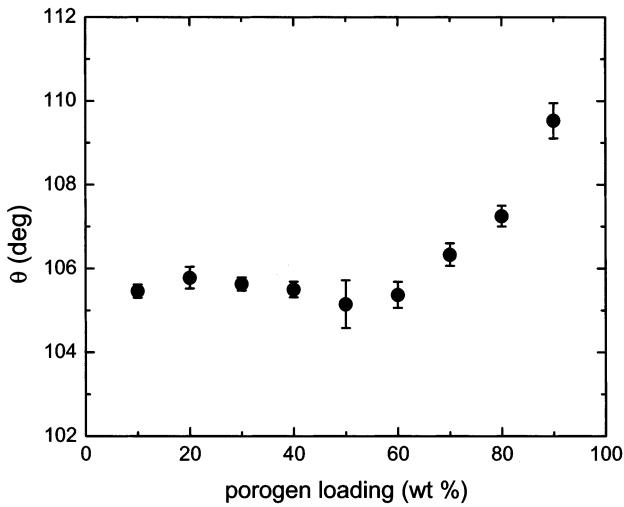


**Figure 4.** Static water contact angles on nanoporous PMSSQ films.

## Results and Discussion

Figure 3 shows a cross-sectional FESEM image of nanoporous PMSSQ with 50 wt % porogen loading. A uniform distribution of nanoscopic pores is observed throughout the entire film thickness. An independent small-angle X-ray scattering (SAXS) study determined the average pore radius of 50 Å with a log-normal type pore size distribution.<sup>12</sup> The surfaces of nanoporous PMSSQ films are hydrophobic as seen by the static water contact angle data in Figure 4. A relatively constant value of the contact angle  $\sim 105^\circ$  was found for the surfaces up to 60 wt % porogen loading. At higher values of porogen loading, the water contact angle increases with increasing porogen amount due to the increase in surface roughness.

The normalized percent sorption of nanoporous PMSSQ for 1-methoxy-2-propanol acetate (PMAc) is presented in Figure 5 as a function of porogen loading. Sorption increases with increasing porogen loading up to  $\sim 70$  wt % porogen loading. A decreased value was measured for 80 wt % porogen loading, which suggests a change in morphology resulting from the higher concentration of porogen, perhaps associated with the structural collapse of nanoscopic pores. As shown in the inset of Figure 5, the refractive index of 80 wt % porogen loaded film deviates from the linear decrease with

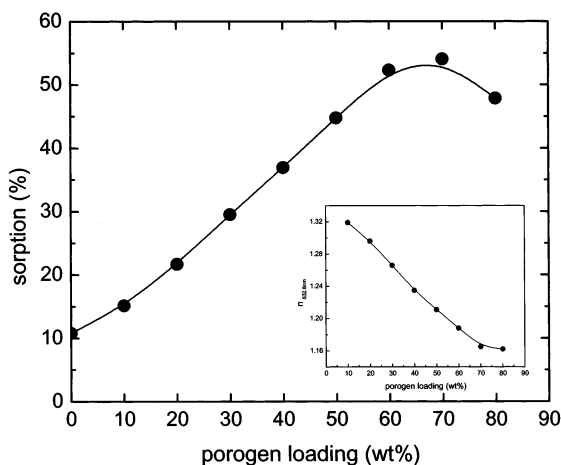


**Figure 5.** Percent sorption of PMAc vs porogen loading plot for nanoporous PMSSQ films. Inset represents the refractive indices of nanoporous films.

porogen loading because the nanoporous film becomes denser by the structural collapse. It is noted that  $\sim 10\%$  sorption was observed for dense PMSSQ without any porogen. This may be attributed to the complex molecular components of the PMSSQ structure (i.e., ladder, cages, branches, etc.), which provide enough free volume for uptake of PMAc molecules.<sup>13</sup> In concept, the presence of a thick adsorbed layer of organic liquid at the surface could also possibly cause the mass change, but an independent neutron reflectivity study with toluene-*d*<sub>8</sub> vapor argues against this possibility because the results show a uniform distribution of toluene throughout the entire film thickness.<sup>14</sup>

Figure 6 shows the reflectance IR spectra of sorption and desorption of PMAc for nanoporous PMSSQ films. The carbonyl group absorption of PMAc (1745  $\text{cm}^{-1}$ ) was monitored throughout the sorption/desorption cycles. For a bare quartz crystal, no carbonyl peak was observed during the sorption cycles, showing that the presence or absence of PMAc vapor in the nitrogen stream flowing through the QCM cell does not produce a detectable change in the IR signal in this study. Strong peaks for the carbonyl group were observed for nanoporous PMSSQ films during the sorption cycle, which disappeared with the start of the desorption cycle. The intensities of the peaks are consistent with extensive accumulation of PMAc within the film in the liquid phase during sorption, congruous with the neutron reflectivity results cited earlier. The steady-state intensity of the carbonyl peak during the sorption cycle increased with increasing porogen loading, confirming enhanced sorption of PMAc into the nanoporous PMSSQ. The IR data also show that the transition between sorption (or desorption) and desorption (or sorption) is rapid, on the order of seconds.

The sorption behavior of the nanoporous PMSSQ containing 50 wt % porogen loading with various organic liquids having different surface tensions is shown in Figure 7. The surface tension, vapor pressure, and density of the liquids are listed in Table 1. Essentially

(12) Huang, E.; Toney, M. F.; Volksen, W.; Mecerreyes, D.; Brock, P.; Lurio, L. B.; Kim, H.-C.; Hawker, C. J.; Hedrick, J. L.; Lee, V. Y.; Magbitang, T.; Miller, R. D. *Appl. Phys. Lett.* **2002**, *81*, 2232.

(13) Baney, R. H.; Itoh, M.; Sakakibara, A.; Suzuki, T. *Chem. Rev.* **1995**, *95*, 1409.

(14) Kim, H.-C.; Huang, E.; Volksen, W.; Miller, R. D.; Yang, G.; Briber, R. M.; Shin, K. W.; Satija, S. K. *Chem. Mater.* submitted for publication.

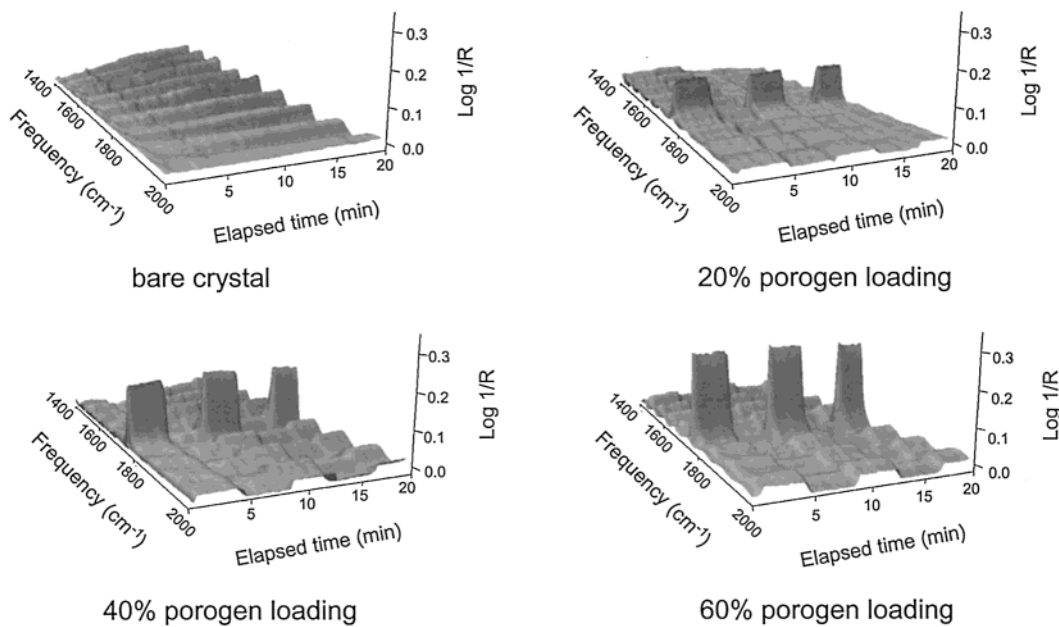


**Figure 6.** Time-dependent IR spectra of nanoporous PMSSQ films during sorption/desorption cycles.

**Table 1. Characteristics of Organic Liquids Used in This Study**

liquids	$\gamma_L$ (dyn/cm)	$P_0$ (mmHg)	density <sup>a</sup> (g/mL)
acetone	23.70	180 @20°C	0.785
methyl isobutyl ketone	23.90	5 @19.7°C	0.801
1-methoxy-2-propanol acetate	26.40	2.8 @20°C	0.968
cyclopentanone	32.80	1.4 @25°C	0.951
benzaldehyde	38.00	1 @26.2°C	1.044
ethylene glycol	47.99	0.06 @20°C	1.113
methylene iodide	50.80	1.5 @21°C	3.325
water	71.99	23.76 @25°C	1.000

<sup>a</sup> At 25 °C.

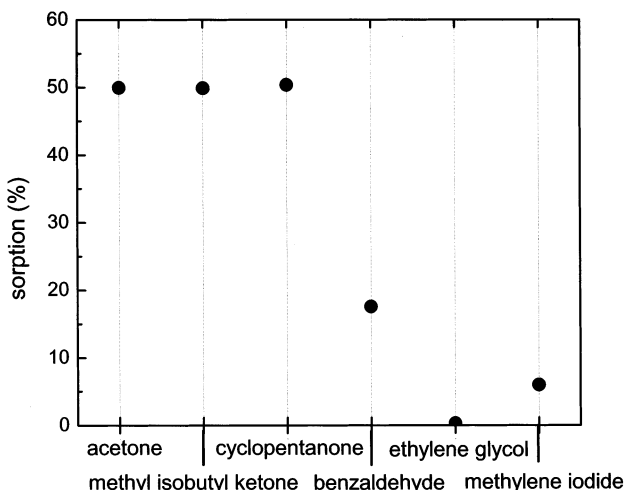


**Figure 7.** Percent sorption of nanoporous PMSSQ films having 50 wt % porogen loading for organic liquids with different surface tensions.

the same amount of sorption (~50%) was measured for acetone, methyl isobutyl ketone, and cyclopentanone. For organic liquids with surface tensions higher than that of benzaldehyde (38.0 dyn/cm), significantly decreased amounts of sorption are observed during the sorption cycles. Because the nitrogen flow carries the vapor of the organic liquids without any pressure buildup in our setup, the molar concentration of the organic liquids in the vapor carried by nitrogen flow varies depending on the vapor pressure of the liquids.

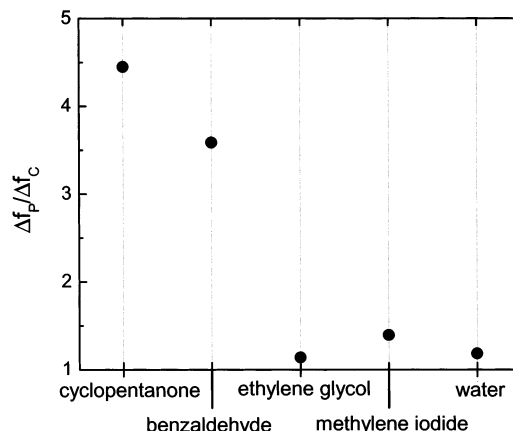


**Figure 8.** Values of  $\Delta f_p/\Delta f_c$  of nanoporous PMSSQ films having 50 wt % porogen loading contacted with liquid phase of organic liquids.

The effect of concentration difference on sorption can be eliminated by immersing the QCM cell in the respective liquid phase of the organic liquids, so that the surface of the nanoporous PMSSQ is in contact with the liquid phase. Figure 8 shows normalized frequency shift ratios of nanoporous PMSSQ with 50 wt % porogen loading for the liquid phase of organic liquids. The frequency shifts of nanoporous films were normalized with respect to the density of pure PMSSQ. The ratios of  $\Delta f_p/\Delta f_c$ , where  $\Delta f_p$  and  $\Delta f_c$  are the frequency differences of nanoporous film and bare quartz crystal between air and liquids, respectively, were measured

**Table 2. Calculated  $P/P_0$  Values for Organic Liquids**

liquid	$\cos \theta^a$	$P/P_0$
acetone	0.9563	0.763
methyl isobutyl ketone	0.9945	0.619
cyclopentanone	0.9659	0.636
benzaldehyde	0.7547	0.624
ethylene glycol	0.0698	0.970
methylene iodide	0.3090	0.815
water	-0.2588	1.056

<sup>a</sup> Contact angles on dense PMSSQ surfaces.

to determine relative sorption amounts of nanoporous films in liquids. The  $\Delta f_p/\Delta f_c$  value approaches 1 when no liquid sorption by the nanoporous films takes place. As shown in the plot, the  $\Delta f_p/\Delta f_c$  values are close to 1 for ethylene glycol, methylene iodide, and water, which means that the amounts of sorption for these liquids are very low. These results suggest that irrespective of the phase (vapor or liquid), the nanoporous PMSSQ films show a selective sorption behavior that depends on the surface tension of the organic liquids. The critical surface tension for sorption was measured to range between 38.0 and 48.0 dyn/cm.

It is interesting to see the spreading criteria for the organic liquids on the PMSSQ surface. The spreading coefficient of a liquid (L) on a solid (S) is given by  $S_{LS} = \gamma_S - (\gamma_L + \gamma_{SL})$ , where  $\gamma_{SL}$  is interfacial tension and  $\gamma_S$  and  $\gamma_L$  are surface tensions of solid and liquid, respectively.  $S_{LS}$  is positive if spreading is accompanied by a decrease in free energy, that is, if it is spontaneous. As the surface tension of PMSSQ as measured by the contact angle with water and methylene iodide is  $\sim 23.7$  dyn/cm, the  $S_{LS}$  values for all of the organic liquids used in this study are negative except for acetone, hence the liquids tend to dewet on PMSSQ surface. This indicates the sorption of nanoporous PMSSQ is not driven by the spontaneous spreading of liquids on PMSSQ surface.

The Kelvin equation can be used to calculate the lowered vapor pressures above capillary-held wetting liquids.<sup>1,15</sup> The relation between the equilibrium vapor pressure ( $P$ ) and the mean radius of curvature ( $r$ ) of a liquid can be described by the equation

$$\ln(P/P_0) = [M/(\rho RT)] \times [(\gamma/r) - (P - P_0)]$$

where  $P_0$  is the saturated vapor pressure,  $M$  is the molecular weight,  $\rho$  is the density,  $\gamma$  is the surface tension of the liquid,  $R$  is the gas constant, and  $T$  is the absolute temperature. The applicability of the equation has been speculated by many workers.<sup>16,17</sup> According to

(15) Thomson, W. *Proc. R. Soc. Edinburgh* **1870**, 7, 63.

(16) Fisher, L. R.; Israelachvili, J. N. *J. Colloid Interface Sci.* **1981**, 80, 528.

(17) Melrose, J. C. *Langmuir* **1989**, 5, 290.

this equation, condensation can take place in small pores ( $r$  is negative) at pressures lower than the normal saturation vapor pressure. For spherical menisci the equation can be simplified to  $\ln(P/P_0) \sim [M/(\rho RT)] \times [(2\gamma \cos \theta)/r_p]$ , where  $\theta$  is the contact angle between the liquid and the pore wall, and  $r_p$  is the mean radius of the pores. Table 2 lists the calculated  $P/P_0$  values for organic liquids in this study using the  $r_p$  value of  $-50$  Å derived from SAXS data. A  $P/P_0$  value of 1.056 is calculated for water, consistent with the extremely low sorption of water observed with nanoporous PMSSQ as the equilibrium vapor pressure in the pores is higher than the normal saturation vapor pressure. All the organic liquids in this study show  $P/P_0$  values less than 1, hence the liquids can condense in the nanoscopic pores at pressures lower than  $P_0$ . The amounts of sorption can be determined by the magnitude of  $P/P_0$  values. As the  $P/P_0$  values for ethylene glycol (0.970) and methylene iodide (0.815) are close to 1, amounts of sorption lower than those of other liquids can be expected. The sorption behavior based on calculations using the Kelvin equation is in good agreement with the experimental sorption data obtained by QCM analysis though the amounts of sorption were determined for a limited time scale of sorption cycles. More detailed studies would be interesting to elucidate the sorption kinetics for different morphologies and pore sizes. The unique sorption selectivity of nanoporous PMSSQ films is expected to open up a number of possibilities for potential applications such as sensors, separation media, and so on.

## Conclusions

The nanoporous PMSSQ thin films prepared by a simple and efficient route show highly selective sorption behavior independent of the phase of organic liquids (liquid or vapor). This phenomenon can be explained by the Kelvin equation that accounts for the capillary condensation of unsaturated vapors. The critical surface tension for sorption of organic liquids was estimated to be in the range from 38.0 to 48.0 dyn/cm.

**Acknowledgment.** We acknowledge K. R. Carter, M. Oye, S. Follonier, and K. K. Kanazawa for their contributions. Financial support by the U.S. National Institute of Standards and Technology (NIST/ATP Cooperative Agreement 70NANB8H4013) is gratefully acknowledged. J.B.W. thanks the Center for Polymer Interfaces and Macromolecular Assemblies (CPIMA) at IBM Almaden Research Center sponsored by NSF-MRSEC (Grant DMR-9808677) and NSF-REU (Grant DMR-9820149).

CM020375E